Published in final edited form as:
Hippocampus. 2012 September ; 22(9): 1848–1859. doi:10.1002/hipo.22019.

Distinct contributions of human hippocampal theta to spatial cognition and anxiety

Brian R. Cornwell[1], **Nicole Arkin**[1], **Cassie Overstreet**[1], **Frederick W. Carver**[2], and **Christian Grillon**[1]

[1]Section on Neurobiology of Fear and Anxiety, National Institute of Mental Health, National Institutes of Health, Bethesda, MD, USA

[2]Magnetoencephalography Core Facility, National Institute of Mental Health, National Institutes of Health, Bethesda, MD, USA

Summary

Current views of the hippocampus assign this structure, and its prominent theta rhythms, a key role in both cognition and affect. We studied this duality of function in humans, where no direct evidence exists. Whole-head magnetoencephalographic (MEG) data were recorded to measure theta activity while healthy participants ($N = 25$) navigated two virtual Morris water mazes, one in which they risked receiving aversive shocks without warning to induce anxiety and one in which they were safe from shocks. Results showed that threat of shock elevated anxiety level and enhanced navigation performance compared to the safe condition. MEG source analyses revealed that improved navigation performance during threat was preferentially associated with increased left septal (posterior) hippocampal theta (specifically 4–8 Hz activity), replicating previous research that emphasizes a predominant role of the septal third of the hippocampus in spatial cognition. Moreover, increased self-reported anxiety during threat was preferentially associated with increased left temporal (anterior) hippocampal theta (specifically 2–6 Hz activity), consistent with this region's involvement in mediating conditioned and innate fear. Supporting contemporary theory, these findings highlight simultaneous involvement of the human hippocampus in spatial cognition and anxiety, and clarify their distinct correlates.

Keywords

anxiety; hippocampus; magnetoencephalography; spatial cognition; theta oscillation; virtual navigation

The hippocampus supports a variety of cognitive-behavioral functions (Eichenbaum, 2004), most notably spatial learning and memory (Buzsaki, 2005; O'Keefe & Nadel, 1978). The hippocampus also figures prominently in affective-motivational states such as anxiety (Gray & McNaughton, 2000; McNaughton et al., 2007); its dysfunction has been implicated in anxiety (Bonne et al., 2008; Karl et al., 2006) and mood disorders (Cornwell et al., 2010; Frodl et al., 2008; Sahay & Ren, 2007). In synthesizing these two distinct bodies of empirical data, some researchers have posited a unitary function for the hippocampus, one that is fundamental to a wide range of cognitive and affective processes (Bland & Oddie, 2001; Davidson & Jarrard, 2004; Gray & McNaughton, 2000). Others have highlighted potential subdivisions of the hippocampus along anatomical and/or spectral (i.e., distinct theta rhythms) lines to account for its diverse functionality (Bannerman et al., 2004;

Corresponding Author: Brian R. Cornwell, National Institute of Mental Health, NIH, 15K North Drive, MSC 2670, Bethesda MD 20892, cornwellb@mail.nih.gov, Phone: 301-402-7219, Fax: 301-594-9959.

Fanselow & Dong, 2010; Shin, 2009). Aside from this theoretical attention, empirical work in rodents focusing simultaneously on contributions of the hippocampus to cognition and affect is relatively scarce, despite some recent exceptions (Bannerman et al., 2003; Bertoglio et al., 2006; Czerniawski et al., 2009; Moita et al., 2004; Royer et al., 2010). To our knowledge, this duality has not been explored in humans.

A functional-anatomical division along the longitudinal axis of the hippocampus provides potential grounding for its dual role in cognition and affect. Septal (or dorsal or posterior) hippocampus has been extensively implicated in spatial cognition (Moser et al., 1993; Moser et al., 1995). The septal third is heavily interconnected to retrosplenial cortices, cingulate cortices and striatal regions (among others), supporting its role in cognitive processes (Fanselow & Dong, 2010). Temporal (or ventral or anterior) hippocampus, in contrast, contributes to anxiety and modulation of stress responses (Kjelstrup et al., 2002; Ohmura et al., 2010; Oler et al., 2010), projecting to structures mediating affective processes such as the amygdala, hypothalamus and medial prefrontal cortices (Fanselow & Dong, 2010; Ishikawa & Nakamura, 2006). Although most of this evidence stems from animal work, human neuroimaging studies have yielded similar insights. For example, spatial cognitive tasks routinely elicit activity in septal hippocampus (Hartley et al., 2003; Maguire et al., 1998; 1999). Contextual fear conditioning studies, on the other hand, find enhanced temporal hippocampal activity in aversive contexts (Alvarez et al, 2008; Hasler et al., 2007; Marshner et al., 2008), although these results could reflect enhanced spatial processing of aversive contexts rather than mediating affective processes *per se*. Despite this emerging picture, no human neuroimaging studies to date have investigated both putative functions simultaneously and explicitly addressed this potential functional-anatomical division. We aimed to fill this gap by focusing on a particular kind of brain oscillation that is central to hippocampal function: theta activity.

Rodent electrophysiological work has long established that hippocampal neuronal populations exhibit theta rhythms (4–12 Hz) under various conditions, predominantly during exploratory behaviors (Buzsaki, 2002; 2005). Hippocampal theta is thought to be essential to spatial learning (McNaughton et al., 2006; Winson, 1978), and episodic memory formation more generally (Buzsaki, 2005). Importantly, two kinds of hippocampal theta, with distinct pharmacological and behavioral profiles (Bland, 1986), may support diverse functions (Shin, 2009). Type-1 theta is non-cholinergically-mediated and observed during locomotion (Bland & Oddie, 2001). Type-2 theta is cholinergically-mediated, and evident during immobile, but highly arousing and vigilant conditions (e.g., presence of predator, Sainsbury et al., 1987). Recently Shin and colleagues dissociated type-1 and type-2 theta genetically with knockout mice characterized by deficient cholinergic signaling in the medial septum (Shin et al., 2009) and hippocampus (Shin et al., 2005). Cholinergic deficiency led to reduced type-2 theta and increased anxiety-like behaviors, but had no effect on type-1 theta (Shin et al., 2009). Given that type-1 and type-2 theta often have different spectral peaks (7–12 and 4–7 Hz, respectively), theta frequency may also be useful to consider, in addition to anatomical location, as a starting point for studying cognitive versus affective functions of the human hippocampus.

Despite being less prominent in humans (Cantero et al., 2003), as well as other primates (Stewart & Fox, 1991), theta activity may, nevertheless, be important for human brain function (Duzel et al., 2010; Kahana et al., 2001). Invasive electrophysiological studies (in epileptic patients) employing virtual reality environments, for instance, have shown that the human hippocampus exhibits theta oscillations (4–8 Hz) during periods of goal-directed navigation (Ekstrom et al. 2005; Caplan et al., 2003). Previously, we found that septal hippocampal theta positively correlated with spatial navigation performance (Cornwell et al., 2008; 2010). In these latter studies, hippocampal theta was measured noninvasively

using whole-head magnetoencephalography (MEG) while participants navigated a virtual analogue of the Morris water maze, a task known to be hippocampal-dependent in both its actual (Morris et al., 1982) and virtual form (Astur et al., 2002; Bartsch et al., 2011; Goodrich-Hunsaker et al., 2010). Research on specifying a role for human hippocampal theta in spatial learning and other cognitive functions, however, has not been matched by similar attention to the potential significance of hippocampal theta for anxiety.

In the current study, we modified the virtual Morris water maze task to extend the significance of human hippocampal theta to anxiety. While undergoing whole-head MEG, participants ($N = 25$) navigated two virtual pools in search of an escape platform, one in which they risked receiving electric shocks before reaching the platform and one in which they were safe from shocks (Figure 1). Threat of unpredictable shocks is a well-validated and powerful method for inducing sustained anxiety (Grillon, 2002). In this experimental task context, cognitive factors underlying spatial learning and affective factors underlying shock anticipation can be quantified independently – using measures of navigation performance and subjective anxiety experience, respectively – and linked to hippocampal theta activity. Based on the literature, we hypothesized two ways in which these potential functional correlates of hippocampal theta could be separated. Anatomically, it was predicted that navigation performance would be associated with septal hippocampal theta (Cornwell et al., 2008, 2010), and anxiety with temporal hippocampal theta (Fanselow & Dong, 2010). Spectrally, we anticipated that cognitive and affective functions of the hippocampus would be distinctly associated with specific theta-frequency bands, with navigation performance linked to high-frequency theta (Cornwell et al., 2008; 2010) and anxiety linked to low-frequency theta (Shin et al., 2009).

Materials and Methods

Participants

Twenty–five healthy, right-handed individuals completed the study (13 men, 12 women, mean age = 29 y, SD = 6 y). Data from six additional participants were excluded because of either excessive head movement during the MEG scans or extremely poor task performance (i.e., > 3 standard deviations of the mean). Exclusion criteria for participation included: (1) past or current psychiatric disorders determined by a Structured Clinical Interview for DSM-IV (First et al., 1995), (2) cardiovascular abnormalities determined by a physical exam, (3) current use of psychoactive medications as per self-report and (4) current use of illicit drugs determined by urinalysis. Participants were screened for non-removable metallic objects that might cause significant artifacts in the MEG (or pose safety concerns in the MRI environment). The study was approved by the Combined Neuroscience Institutional Review Board of the National Institutes of Health. All participants gave informed consent in writing prior to participation and received monetary compensation.

Electrode set-up

Two surface electrodes were attached to the left wrist for shock administration by a Grass S88 constant voltage stimulator (Astro-Med, Inc., RI, USA). A third surface electrode attached to the forearm served as ground. Before participants were placed in the MEG scanner, shock intensity was set individually for each participant to a level reported to be moderately uncomfortable. Participants were informed that they could receive 5−15 shocks during the recordings. Ten shocks (5 per run) were delivered.

virtual Morris water maze task

The virtual Morris water maze task was administered with commercial software (http://www.neuroinvestigations.com). Participants completed two runs of 40 trials, using

their right (dominant) hand to navigate the virtual pool with a custom-made fiber-optic joystick (Figure 1). During both runs, participants alternated every fifth trial between two pools, one in which they were at risk to receive shocks at any time they were not on the platform (threat) and one in which they were safe at all times (safe). Each pool could be identified by the distal cues on the surrounding walls (i.e., objects such as a window or door in one pool and abstract paintings in the other), and participants were instructed so before the MEG recordings. Other than the distal cues, the pools were structurally identical. The assignment of pools to threat and safe conditions, as well as the order of conditions, was counterbalanced across participants. For the threat condition, shocks were delivered randomly on 5 of 20 trials for each run, at least 2.5 s after trial onset but before participants had reached the platform.

In the first run (visible platform condition, encoding phase), the platform was visible above the water in a fixed location and participants navigated to it 40 times (20 times per pool context) from one of four starting points at the pool's edge (pseudo-randomly ordered). Each trial began with the participant facing the edge, requiring them to turn around to view the entire pool layout. In the second run (hidden platform condition, retrieval phase), the platform was submerged for 15 s in the same fixed location as in the first run and participants navigated to it 40 times (20 times per pool) from the same four starting points. Because the platform was hidden, participants had to use the distal visual cues to navigate efficiently. For both runs, participants were instructed to navigate as quickly and directly as possible to the platform, whether visible or hidden. In the hidden platform condition, the platform was raised on trials in which it was not found within 15 s and considered a failed attempt. There was a fixed 2-s inter-trial interval in which a black screen was presented.

MEG and MRI acquisition

Neuromagnetic activity was measured with a CTF-OMEGA 275-channel (first-order gradiometers) whole-head magnetometer (VSM MedTech, Ltd., Canada) in a magnetically-shielded room (Vacuumschmelze, Germany). Synthetic third gradient balancing was used for active noise cancellation. Magnetic flux density was digitized at 1200 Hz with a bandwidth of 0–300 Hz and notch filter at 60 Hz. Fiducial coils were attached to the nasion and right and left preauricular sites. Coils were energized continuously to provide real-time head position in the dewar for later co-registration with the anatomical MRI. Participants who deviated more than 5 mm from their initial head position were excluded. Magnetic resonance images (MRI) were obtained in a separate session using a 3-Tesla whole-body scanner (GE Signa, WI, USA). A high resolution T1-weighted (magnetization-prepared rapid-acquisition gradient echo [MPRAGE]) MRI was obtained from each participant with radiological markers (IZI Medical Products Corp, MD, USA) attached to the same three fiducial sites to facilitate spatial coregistration.

Subjective anxiety assessment

Following each run, participants were asked to rate their anxiety level during threat and safe conditions. A 0–10 scale was used, ranging from "no anxiety" to "extreme anxiety." To compare self-reported anxiety level across conditions, a two-way repeated-measures ANOVA on angular transformed values was performed (using arcsin x^{-1}, where×is the raw anxiety score expressed as a proportion).

Navigation performance assessment

The virtual Morris water maze software performs automated calculations of multiple variables for assessing trial-by-trial performance, including latency to reach the platform, path length to the platform and heading error. These measures are typically correlated; in the present sample, for instance, mean path length and mean heading error show a strong

positive correlation between subjects (Pearson *r*'s = .67 and .90 for the threat and safe conditions, respectively). To compare performance between conditions, latency and path length were not considered because we imposed a 15-s time limit on hidden platform trials – to avoid fatigue in the MEG scanner – which significantly reduced the range of possible values for these two variables.

Our primary measure was heading error, which is a point estimate of the angular deviation between the current path and the ideal path (i.e., straight line). Heading error is recorded early, specifically at the point in which the participant has traversed 25% of the pool's diameter; it is therefore not influenced by trial duration. Importantly, the initial trajectory taken by the participant, which heading error estimates, is thought to rely strongly on the use of distal environmental cues when the platform is hidden (Woolley et al., 2010), and thus may be a particularly sensitive measure of hippocampal function. Mean heading error was calculated for each block of 4 trials, square-root transformed, and entered into a 2 (condition) × 5 (block) repeated-measures ANOVA. For comparing overall performance between conditions on hidden platform trials, we performed a paired *t* test on the number of failed attempts (out of 20 trials) to reach the platform within the allotted 15 s.

Time-frequency analyses

The Stockwell transform (Stockwell et al., 1996) was applied to raw MEG sensor data to determine the dominant spectral changes occurring in the first 2 s relative to trial onset for the 20 hidden trials. Detailed topographic information was not important for this purpose, and thus sensors overlying temporal cortices were averaged for each hemisphere. Custom software (freely available at http://kurage.nimh.nih.gov) was used for Stockwell analyses and plotting. For plotting, these data were normalized to power within a 1-s baseline window immediately preceding trial onset.

Synthetic Aperture Magnetometry (SAM)

SAM is a minimum-variance adaptive beamformer algorithm for estimating source power within specific time and frequency windows across the brain with no *a priori* assumptions about the number of active sources or their spatial locations (Hillebrand et al., 2005; Vrba & Robinson, 2001). In general, source space is parsed into a 3-dimensional grid with an optimum spatial filter specified for each grid point ("voxel"). A spatial filter or beamformer is essentially a weighted linear combination of sensor data, where the weight vector at each grid point is derived from the signal covariance of unaveraged sensor data digitally filtered in a frequency band of interest. Interfering sources, neural as well as artifactual ones of ocular and muscular origin, are suppressed by minimizing the output of the spatial filter. Signal from the target location is retained by constraining the lower bound of minimization to unity gain for a dipolar current source, which is obtained by calculating the biomagnetic forward solution with a multiple-sphere source-space model (derived from the anatomical MRIs). Localizing hippocampal activity with adaptive MEG beamformers has been successful across multiple experimental paradigms (Cornwell et al., 2008; 2010; Moses et al., 2009; Quraan et al., 2010; Riggs et al., 2009).

SAM analyses were carried out on two partially overlapping low-frequency bands: 4–8 Hz and 2–6 Hz. In our previous studies using the virtual Morris water maze, we defined theta activity exclusively by the 4–8 Hz band (Cornwell et al., 2008; 2010). In light of the possible functional distinction between different theta-frequency bands (Shin et al., 2009), here we also estimated power in the 2–6 Hz band, which spans the traditional boundary between theta and delta oscillatory activity. Intracranial EEG studies report that delta as well as theta oscillations are present in the human hippocampus, and may function similarly (Jacobs et al., 2007; Lega et al., 2011; Mormann et al., 2008). Moreover, Stockwell time-

frequency plots motivated the selection of 4–8 Hz and 2–6 Hz bands. Although these bands overlap, they should nevertheless be relatively sensitive to higher versus lower theta activity, respectively. For the remainder of the manuscript, we refer to 4–8 Hz activity as high-frequency (or high) theta and 2–6 Hz activity as low-frequency (or low) theta.

Source analyses focused on the first 2 s of each trial for several reasons. First, hippocampal theta does not appear for extended periods in humans (Cantero et al., 2003), and we have had previous success localizing hippocampal theta at the start of navigation (Cornwell et al., 2008). Second, to be able to use all of the 20 trials in the visible and hidden platform runs for SAM analyses, we were constrained by 5 trials containing shocks (delivered as early as 2.5 s relative to trial onset), which could systematically influence oscillatory activity during threat. Third, we wanted to capture activity preceding movements before calculation of heading errors, the primary measure of performance used here; based on mean latencies to first movements, most participants took longer than 2 s on average to begin navigating.

Source power was estimated for five time windows relative to trial onset (0.00–1.00 s, 0.25–1.25 s, 0.50–1.50 s, 0.75–1.75 s and 1.00–2.00 s). All 1-s active windows were compared to the same 1-s baseline window before trial onset in the inter-trial interval. This yields a metric of relative power (pseudo-F ratio) with positive values indicating increased power relative to baseline and negative values decreased power. Each individual SAM source image consisted of a volume of pseudo-F power ratios with a spatial sampling of 5 mm (voxel size = 5 mm^3). We should note that the alternative of performing a single analysis over the 2-s window is not optimal given that it would require a control condition of similar length for a balanced comparison, and the entire 2-s intertrial interval, which includes event-related activity associated with the offset of the previous trial, would not be an appropriate baseline state for this comparison.

Weight vector correlation analyses

Before performing group analyses, we addressed the orthogonality of the beamformers for temporal and septal thirds of the hippocampus to validate that there was sufficient independence in the estimates of theta activity between these subregions to test our main hypotheses. This was achieved by performing correlation tests of weight vectors between the beamformers specifying the temporal third and those specifying the septal third, for both the left and right hippocampus (for a similar approach to estimating the spatial resolution of adaptive beamformer analyses, see Barnes et al., 2004). Weight vectors were extracted for correlation tests from the voxel within each subregion (see next section) at the boundary closest to the other subregion (i.e., most anterior voxel in the septal third vs. most posterior voxel in the temporal third). Results were analyzed in terms of the shared variance (coefficient of determination, r^2) between (left or right) temporal and septal hippocampus.

Group Statistical Analyses – regression analyses

Using AFNI (Cox, 1996), SAM images for each condition, time window and frequency band were manually spatially warped to a Talairach brain template to allow for group analysis in a standardized source space, and within-volume normalized (z-score transformation) to limit the influence of global signal power differences between participants on local source power comparisons. To address the relationships between hippocampal theta, anxiety and navigation performance, theta power estimates were averaged over anatomically-defined regions of interest (ROIs) and extracted for analysis in SPSS 18. Bilateral masks of the hippocampi were created from the automated Talairach Atlas Daemon (Lancaster et al., 2000) and resampled to the SAM imaging data (5-mm grid). Each voxel retained for the resampled mask overlapped the original mask by at least 10%. This resulted in bilateral masks containing 20 voxels each. Temporal and septal thirds of

each hippocampus were averaged separately based on the location of each voxel along the coronal axis: for temporal, y > −20, and for septal, y < −29. Voxels situated in the intermediate third of each hippocampus were discarded from these averages to maximize independent estimation of temporal and septal hippocampal theta source power.

Hierarchical multiple regression analyses were conducted to determine relationships between hippocampal ROI theta and navigation performance (mean heading error) and anxiety level. Differential values were computed for all variables (threat – safety) to address whether relative effects of threat on navigation performance and anxiety are explained by relative changes in hippocampal theta. Left and right hippocampal theta were analyzed separately to guard against overfitting the regression models in light of the modest sample size (N=25). We did not aim to directly compare left vs. right hippocampal theta.

Preliminary analyses revealed similar Pearson correlations for different time windows, and thus, hippocampal ROI theta power was averaged across time windows to simplify and increase signal-to-noise. Because these are overlapping time windows, this also served to emphasize the middle of the 2-s interval, which is consistent with the timing of theta power changes observed in the time-frequency data from sensors overlying temporal cortices. Two regression models (left and right) were run to determine whether differential septal hippocampal ROI theta on hidden platform trials predicted differential navigation performance. Four regression models were run to determine the extent to which temporal hippocampal ROI theta predicted anxiety level during the hidden and visible platform conditions. Each model contained four predictor variables entered in one step: 2 regions (temporal, septal) by 2 theta bands (4–8 Hz, 2–6 Hz). Diagnostic tests confirmed the absence of significant outliers (> 3 standard deviations) or high degrees of multi-collinearity for all models. Variance inflation factors (VIF) are reported for significant regression coefficients.

To address the relative contribution of septal vs. temporal hippocampal theta to the various model fits, we separately removed septal low and high theta or temporal low and high theta and compared the full model to each of these nested models. Change statistics (ΔR^2) were computed to determine whether exclusion of one set of predictors or another significantly reduced explained variance in differential navigation performance or differential anxiety level.

Results

Threat-induced anxiety response

A 2 × 2 repeated-measures ANOVA on retrospective reports of anxiety revealed a main effect of Condition, $F(1,24) = 92.08$, $p < .001$, indicating greater anxiety reported during threat (mean ± SD, .77 ± .31 transformed arbitrary units) than safe (.33 ± .23) , as well as a Condition by Run interaction, $F(1,24) = 4.87$, $p = .04$. This interaction reflects a greater effect size for the threat manipulation for the visible platform run, $F(1,24) = 83.74$, $p < .001$, partial $\eta^2 = .78$, relative to the hidden platform run, $F(1,24) = 41.98$, $p < .001$, partial $\eta^2 = .64$. While one subject reported no difference in anxiety between conditions in the visible platform run, five subjects did so in the hidden platform run. No subjects reported greater anxiety during safe relative to threat.

Contextual differences in navigation performance

Mean heading error (square-root transformed) was significantly smaller (i.e., better performance) during threat compared to safety when the platform was hidden, $F(1, 24) = 5.03$, $p = .03$ (Figure 2). This effect grew progressively over successive blocks as evidenced by a significant Context-by-Block interaction, $F(4,96) = 2.85$, $p = .03$, and a strong linear decrease across blocks for threat, $F_{linear}(1,24) = 18.51$, $p < .001$, partial $\eta^2 = .44$, but not for

safe, $F_{linear} < 1$, partial $\eta^2 = .02$. When the platform was visible, there was a statistical trend toward a smaller mean heading error during threat compared to safe conditions, $F(1, 24) = 3.02$, $p = .095$, and no evidence of a Context-by-Block interaction, $F(4, 81.8) = 1.43$, Greenhouse-Geisser correction = .85, $p > .23$. Participants did not differ, overall, in their number of failed attempts to reach the hidden platform within 15 s, before it became visible, during threat (Mean ± SD, 6.7 ± 4.7 trials, out of 20 total) vs. safety (7.4 ± 4.8 trials), $t(24) = -1.28$, $p > .10$.

Time-frequency decomposition of navigation-related MEG activity

Stockwell transforms were applied to the MEG sensor data to identify spectral differences in induced power between threat and safe conditions (Figure 3). The first 2 s across 20 hidden platform trials were analyzed. Threat-safe differences in theta/delta activity were prominent during this early interval in the group-averaged spectrograms for sensors overlying left and right temporal cortices. Over the left temporal cortex, there were clear peaks at about 6.4 Hz and 2.2 Hz. Over the right temporal cortex, there was a single main peak around 2.1 Hz. Hippocampal source analyses attempted to capture these distinct differences in high (4–8 Hz) versus low theta (2–6 Hz). Because our primary goal was to link theta activity to navigation performance and anxiety, no other frequency bands were studied further.

Orthogonality of septal and temporal hippocampal beamformers

To validate that there was sufficient independence between the beamformers estimating theta activity for septal and temporal hippocampus, weight vector correlations were computed. Correlation analyses for each run, (hidden platform, visible platform), context (threat, safe), frequency band (4–8 Hz, 2–6 Hz) and time window revealed very little overlap, on average, between septal and temporal hippocampal beamformers, with never more than 7% shared variance (i.e., $r^2 \leq .07$) for the left hippocampus and the right hippocampus. For each participant, there were no cases in which septal and temporal beamformers exhibited > 25% shared variance, suggesting very little overlap in septal vs. temporal theta power estimates.

Septal (posterior) hippocampal theta predicts navigation performance

The first two regression models were run to determine whether differential (threat – safe) septal hippocampal theta at trial onset on hidden platform trials predicted differential navigation performance. Is the relative advantage in navigation performance under threat predicted by a relative increase of theta in the septal third of the hippocampus? For the left hippocampus, the full model fit for differential heading error regressed on differential theta in the hidden platform condition was significant, $F(4,20) = 3.36$, $p = .029$, adjusted $R^2 = .28$. Two predictors, left septal high theta (4–8 Hz) and left septal low theta (2–6 Hz), showed significant, but opposite, relationships to differential heading error, $t(20) = -3.20$, $p = .005$, $\beta = -.63$, partial $r = -.58$, VIF = 1.29 and $t(20) = 2.15$, $p = .04$, $\beta = .45$, partial $r = .43$, $VIF = 1.43$, respectively. Across participants, as differential high theta (4–8 Hz) in the septal third of the left hippocampus increases under threat of shock (relative to safety, Figure 4), and differential low theta (2–6 Hz) in the same region decreases, navigation performance improves (Note that smaller heading errors reflect more accurate trajectories.). For the right hippocampus, differential theta was not significantly related to differential heading error, $F(4,20) = 1.22$, $p > .05$, adjusted $R^2 = .04$.

To compare the relative predictive value of differential theta in the septal third of the left hippocampus over theta in the temporal third, we used hierarchical regression analyses to examine changes in fit (R^2) between the full model and two alternative simpler models (left septal theta only, left temporal theta only). There was no difference in model fit between the nested model including septal high and low theta only and the full model for differential left

hippocampal theta, $\Delta R^2 = .05$, $\Delta F(2, 20) < 1$, $p > .05$. In contrast, the full model did perform significantly better than the nested model including temporal high and low theta only, $\Delta R^2 = .33$, $\Delta F(2, 20) = 5.53$, $p = .01$. These results indicate that differential left temporal hippocampal theta has little predictive value for differential navigation performance compared to differential left septal hippocampal theta.

Temporal (anterior) hippocampal theta indexes anxiety level

The next two regression models were run to determine whether differential temporal hippocampal theta predicted differential anxiety on hidden platform trials. Is the relative increase in anxiety under threat marked by a relative increase of theta in the temporal third of the hippocampus? For the left hippocampus, the full model fit for differential anxiety level regressed on differential theta in the hidden platform condition was significant, $F(4,20) = 3.20$, $p = .035$, adjusted $R^2 = .27$. One predictor, left temporal low theta (2–6 Hz), showed a significant positive relationship with anxiety level, $t(20) = 3.19$, $p = .005$, $\beta = .62$, partial $r = .58$, $VIF = 1.23$. This result suggests that as differential low theta (2–6 Hz) increases in the temporal third of the left hippocampus under threat of shock (relative to safety), self-reported anxiety increases (Figure 4). For the right hippocampus, differential theta was not significantly related to differential anxiety level, $F(4,20) = 2.03$, $p > .05$, adjusted $R^2 = .15$.

Hierarchical analyses indicated no difference in model fit between the nested model including only left temporal high and low theta and the full model for differential left hippocampal theta, $\Delta R^2 = .15$, $\Delta F(2, 20) = 2.51$, $p > .05$. The full model, in contrast, did perform significantly better than the nested model including only septal high and low theta, $\Delta R^2 = .31$, $\Delta F(2, 20) = 5.15$, $p = .02$. Thus, differential left septal hippocampal theta has little predictive value for differential anxiety compared to differential left temporal hippocampal theta.

Two final regression models were run to determine whether differential temporal hippocampal theta predicts differential anxiety on visible platform trials. Full model fits for differential anxiety level regressed on differential left hippocampal theta and differential right hippocampal theta were not significant, $F < 1$, adjusted $R^2 = -.14$ and $F(4,20) = 2.37$, $p > .05$, adjusted $R^2 = .19$, respectively.

Discussion

Virtual navigation provides fertile ground to study hippocampal functioning in humans (Burgess et al., 2002). Here, we measured whole-head MEG while participants navigated two virtual Morris water mazes, one of which was made aversive by the threat of shock, to study contributions of human hippocampal theta to spatial cognition and anxiety (Figure 1). Our results support links to both processes. Of central significance, relationships between left hippocampal theta and navigation performance on the one hand, and anxiety on the other hand, were anatomically distinct (septal vs. temporal regions, respectively) and spectrally distinct (high-frequency [4–8 Hz] vs. low-frequency [2–6 Hz] theta activity, respectively). These findings support theoretical accounts of hippocampal function in rodents that postulate involvement of the hippocampus in both cognitive and affective processes (Bannerman et al., 2004; Davidson & Jarrard, 2004; Fanselow & Dong, 2010; Gray & McNaughton, 2000). They extend this proposed duality of function to the human hippocampus, and clarify distinct correlates of cognition- and anxiety-related hippocampal activity.

Threat of shock increased participants' anxiety and improved their navigation performance (Figure 2). This latter effect is indicated by heading error measurements; participants were more accurate in their initial trajectories to the hidden platform during threat than safety.

Mean heading error was different only when the platform was hidden, not when the platform was visible, and this difference between conditions on hidden trials grew over successive trial blocks. Threatening conditions thus enhanced the rate of spatial learning – in terms of participants' taking increasingly accurate trajectories to the platform – which in turn may reflect greater processing of distal environmental cues to guide navigation (Woolley et al., 2010). However, there was no overall difference between conditions in the number of failed attempts to find the hidden platform, suggesting that threat of shock had only modest beneficial effects on navigation performance. It is worth noting that because anxious arousal and behavioral performance may not be monotonically related (Salehi et al., 2010; Yerkes & Dodson, 1908), higher anxiety levels could produce detrimental effects on performance. This might have implications for separating cognition- and anxiety-related functions of hippocampal theta as presented below.

In two past studies, we found a positive correlation between left septal (posterior) hippocampal theta (4–8 Hz) and navigation performance (Cornwell et al., 2008; 2010). A similar relationship emerged in the present data (Figure 4). Across participants, as high theta (4–8 Hz) in the septal third of the left hippocampus increased during threat relative to safety, relative performance improved (i.e., smaller heading errors under threat relative to safety). In contrast, low theta (2–6 Hz) in the left septal hippocampus was negatively associated with navigation performance, suggesting that high theta, especially, is beneficial for encoding one's initial location in the virtual pool and for selecting accurate trajectories to the hidden platform. This observation highlights the potential spectral specificity of left septal hippocampal theta in mediating these cognitive processes; however, whether low frequency theta (or delta activity) in the left septal hippocampus is actually detrimental to spatial navigation performance will require replication.

We found no evidence to suggest that temporal (anterior) hippocampal theta was related to navigation performance, which is consistent with previous findings (Cornwell et al., 2008; 2010), and suggests a preferential involvement of left septal hippocampal theta in spatial cognition. A functional role for the temporal hippocampus cannot be dismissed, however. Although temporal hippocampal lesions have little consequence for spatial learning in rodents – unlike septal lesions that lead to profound deficits (Moser et al., 1993; Moser et al., 1995) – temporal hippocampal neurons do show place fields (albeit, coarser than septal neurons) and other features that are consistent with a role in spatial processes (Fortin et al., 2008; Jung et al., 1994; Kjelstrup et al., 2008; Royer et al., 2010). In humans, the temporal hippocampus may play a role in initial spatial encoding (Cornwell et al., 2008; Wolbers & Büchel, 2005) and other kinds of early learning processes such as forming visual associations (Woollett & Maguire, 2009). Instead of having strict compartmentalization of spatial cognitive functions, the hippocampus may therefore show a functional gradient along its longitudinal axis (Royer et al., 2010). Nevertheless, the relative importance of theta in the septal third of the hippocampus for accurate spatial navigation is further bolstered by the present results.

Consistent with a role of the hippocampus in affective processes, we found that low theta (2–6 Hz) in the temporal third of the left hippocampus showed a positive correlation with self-reported anxiety, such that those who were most anxious while navigating during threat relative to safe conditions showed the highest increases in low theta in this region during threat (Figure 4). This was neither the case for high theta in the temporal third nor theta in septal third of the left hippocampus, thus indicating both regional and spectral specificity in the link between left temporal hippocampal theta and anxiety. Anxiety-related temporal hippocampal theta is consistent with the preponderance of human neuroimaging studies reporting elevated temporal hippocampal activity (as opposed to septal activity) in aversive, anxiety-provoking contexts (Alvarez et al., 2008; Hasler et al., 2007; Marshner et al., 2008).

Two principal anatomical targets of the temporal hippocampus that underscore its involvement in affective processes are the amygdala and medial prefrontal cortices (Ishikawa & Nakamura, 2006). Recording from the lateral amygdala and CA1 region of the hippocampus, (Seidenbecher et al 2003) found synchronized theta activity between these two structures during fear conditioning when rodents were exposed to a stimulus that was associated with shock delivery (also see Pape et al., 2005). Aversive learning may therefore involve theta-mediated interaction of the temporal hippocampus and amygdala. Moreover, hippocampal theta oscillations increase along with anxiety-like behaviors in genetically-engineered mice having serotonin 1A receptor deficiencies (Gordon et al., 2005). Further work with this knockout model shows that theta oscillations in medial prefrontal regions, particularly during anxiety-provoking conditions, are synchronized with those in the temporal hippocampus but not the septal hippocampus (Adhikari et al., 2010). Our data are consistent with this regional specificity, and provide the first evidence of a link between temporal hippocampal theta and anxiety in humans.

It is also noteworthy that anxiety-related activity in the left temporal hippocampus was restricted to low (2–6 Hz) theta. In rodents, cholinergically-mediated type-2 theta is typically slower in frequency (4–7 Hz) than non-cholinergically-mediated type-1 theta (7–12 Hz); and the former has been linked to anxiety-like behaviors (Sainsbury et al., 1987; Shin et al., 2009). It is tempting to interpret the present data similarly, that is, as showing a specific relationship between type-2 theta in the left temporal hippocampus and anxiety. Drawing this comparison is too speculative, however, and there are important exceptions to the observation that type-1 and type-2 theta are spectrally distinct (McNaughton & Sedgwick, 1978; Sainsbury & Montoya, 1984; Vanderwolf, 1975). It does raise important questions about whether low or high theta can be modulated by cholinergic agents and thus whether the two theta bands studied here can be pharmacologically dissociated. This would be an important avenue to pursue. To the extent that human hippocampal theta can be linked to cholinergic processes, these findings may provide potential grounding of mechanisms that underlie the anxiolytic effects of cholinergic antagonists such as scopolamine (Furey et al., 2010).

In contrast to the relationships found between left hippocampal theta and navigation performance and anxiety, no evidence emerged in the right hippocampus. This is surprising in light of the well-established role of the right hippocampus in spatial processes (Burgess et al., 2002). However, these results are consistent with our previous findings for human hippocampal theta (Cornwell et al., 2008; 2010; also see de Araújo et al., 2002), and in a recent human intracranial EEG study specifically investigating lateralized oscillatory patterns during navigation, hippocampal theta was not found to be lateralized (Jacobs et al., 2010). Several factors could be contributing the leftward bias in our data. From a sensorimotor perspective of hippocampal theta (Bland & Oddie, 2001), right-lateralized manual control of navigation in this task could be engaging contralateral structures more than ipsilateral ones. The slight gender bias in our sample (13 men, 12 women) may also be a contributing factor, given evidence that the left hippocampus may be recruited more strongly in men than women (Grön et al., 2000). Moreover, this null result for the right hippocampus could be a consequence of our focus on the first 2 s of each trial, when participants were generally still, given evidence that the right septal hippocampus may play an ongoing role in active navigation but less so during early periods (Xu et al., 2010).

More theoretically interesting, our results could be driven by the kind of spatial cognitive strategies employed, which has been shown to be influenced by acute stress (Schwabe et al., 2007), and how central a role episodic memory retrieval plays in navigating (Burgess et al., 2002). Along these lines, Iglói and colleagues (2010) present fMRI evidence indicating that map-based navigation (allocentric spatial processing) recruits the right hippocampus while

route-based navigation (sequential egocentric spatial processing) activates the left hippocampus. Although there are no structurally-defined routes to follow in the virtual pool (like in a T-maze or Starmaze), participants repeatedly navigated to the hidden platform from four starting points, the same starting points during training on the visible platform trials. This repetition could have promoted the use of sequential egocentric spatial knowledge to guide navigation to the hidden platform. Accordingly, procedural modifications that force generation of novel routes may be critical to shifting participants to a map-based allocentric strategy that might entail greater recruitment of the right hippocampus.

Regarding the absence of anxiety-related right hippocampal theta activity, previous neuroimaging data provide a mixed picture of left (Marshner et al., 2008) versus right (Alvarez et al., 2008; Hasler et al., 2007) hippocampal involvement in aversive contexts; animal research rarely addresses questions of lateralized hippocampal function (Klur et al., 2009). It is therefore unclear whether the leftward bias for temporal low theta is meaningful or stems from low statistical power. For instance, it is possible that the predominant use of a sequential egocentric strategy to navigate could result in mediation of other functions to the left hippocampus, including the processing of affective features of the environment. This may have facilitated retrieval of episodic knowledge related to previous shock delivery (Gomez et al., 2009), being particularly prominent in the more anxious participants.

Finally, while our focus here was to investigate cognitive and affective roles of distinct theta bands without regard to the exact timing of these responses, group-averaged time-frequency plots of sensor data indicate a differential temporal response: high theta peaking between 500 and 750 ms and low theta peaking between 1000 and 1750 ms (Figure 3). Based on how the first few seconds of each trial typically unfold, the relative timing of these theta-band responses may also reflect on their potential functional roles. At trial onset, participants faced the pool's edge with limited visual access to the distal cues surrounding the pool (i.e., one cue was visible). The early high-frequency theta might facilitate spatial orienting by pattern completion when one's position is relatively ambiguous. The subsequent low-frequency theta appears (roughly) as participants turn from the pool's edge and its layout comes into full view. This response could be related to retrieval of specific episodic memory traces, including spatio-temporal features of previous shock delivery. These interpretations are tentative given the complexity of processes underlying spatial navigation and the behavioral variability across trials and individuals. A more detailed investigation of the temporal courses of distinct theta-band activity may provide further insight into their functional differentiation.

To summarize, we present data indicating a role for the human hippocampus in both spatial cognition and anxiety. Clear evidence for these distinct functional correlates was observed in the left hippocampus, indicating that the septal (posterior) third is preferentially involved in spatial cognition while the temporal (anterior) third is involved in anxiety. A further distinction emerged between high (4–8 Hz) theta activity underlying better navigation performance and low (2–6 Hz) theta activity underlying self-reported anxiety level. Pharmacological investigations with cholinergic compounds are needed to address whether these two theta signals are functionally homologous to type-1 and type-2 theta in rodents. It should also be recognized that the anatomical and spectral dissociations reported here should be considered quantitative and do not necessarily reflect qualitatively different functions. As alluded to earlier, a potential non-monotonic relationship between anxious arousal and cognitive performance might indicate a more complex set of underlying mechanisms that was not fully illuminated here. Nevertheless, these findings should foster more precise hypotheses of hippocampal function and dysfunction in conditions ranging from posttraumatic stress disorder (Bonne et al., 2008) to Alzheimer's disease (Henneman et al.,

2009). Equally provocative, these distinct relationships of hippocampal theta should help specify targets for evaluating the efficacy of both candidate anxiolytics and pro-cognitive compounds *in humans* (McNaughton et al., 2007).

Acknowledgments

This research was supported by the Intramural Research Program of the National Institute of Mental Health, National Institutes of Health. This study utilized the high-performance computational capabilities of the Biowulf PC/Linux cluster at the National Institutes of Health, Bethesda MD. http://biowulf.nih.gov. We wish to thank Daniel Pine for helpful comments on an earlier draft and the NIMH MEG Core Facility for technical assistance. We also thank Dave Luckenbaugh for his statistical advice. All authors declare no competing financial interests.

References

Adhikari A, Topiwala MA, Gordon JA. Synchronized activity between the ventral hippocampus and the medial prefrontal cortex during anxiety. Neuron. 2010; 65:257–269. [PubMed: 20152131]

Alvarez RP, Biggs A, Chen G, Pine DS, Grillon C. Contextual fear conditioning in humans: Cortical-hippocampal and amygdala contributions. J Neurosci. 2008; 28(24):6211–6219. [PubMed: 18550763]

Astur RS, Taylor LB, Mamelak AN, Philpott L, Sutherland RJ. Humans with hippocampus damage display severe spatial memory impairments in a virtual Morris water task. Behav Brain Res. 2002; 132:77–84. [PubMed: 11853860]

Bannerman DM, Grubb M, Deacon RM, Yee BK, Feldon J, Rawlins JN. Ventral hippocampal lesions affect anxiety but not spatial learning. Behav Brain Res. 2003; 139:197–213. [PubMed: 12642189]

Bannerman DM, Rawlins JNP, McHugh SB, Deacon RMJ, Yee BK, Bast T, Zhang W-N, Pothuizen HHJ, Feldon J. Regional dissociations within the hippocampus – memory and anxiety. Neurosci Biobehav Rev. 2004; 28(3):273–283. [PubMed: 15225971]

Barnes GR, Hillebrand A, Fawcett IP, Singh KD. Realistic spatial sampling for MEG beamformer images. Hum Brain Mapp. 2004; 23:120–127. [PubMed: 15340934]

Bartsch T, Schonfeld R, Muller FJ, Alfke K, Leplow B, Aldenhoff J, Deuschl G, Koch JM. Focal lesions of human hippocampal CA1 neurons in transient global amnesia impair place memory. Science. 2011; 328:1412–1415. [PubMed: 20538952]

Bertoglio LJ, Joca SRL, Guimaraes FS. Further evidence that anxiety and memory are regionally dissociated within the hippocampus. Behav Brain Res. 2006; 175:183–188. [PubMed: 16996146]

Bland BH. Physiology and pharmacology of hippocampal formation theta rhythms. Prog Neurobiol. 1986; 26:1–54. [PubMed: 2870537]

Bland BH, Oddie SD. Theta band oscillation and synchrony in the hippocampal formation and associated structures: the case for its role in sensorimotor integration. Behav Brain Res. 2001; 127:119–136. [PubMed: 11718888]

Bonne O, Vythilingam M, Inagaki M, Wood S, Neumeister A, Nugent AC, Snow J, Luckenbaugh DA, Bain EE, Drevets WC, Charney DS. Reduced posterior hippocampal volume in posttraumatic stress disorder. J Clin Psychiatry. 2008; 69(7):1087–1091. [PubMed: 18572983]

Burgess N, Maguire EA, O'Keefe J. The human hippocampus and spatial and episodic memory. Neuron. 2002; 35(4):625–641. [PubMed: 12194864]

Buzsaki G. Theta oscillations in the hippocampus. Neuron. 2002; 33(3):325–340. [PubMed: 11832222]

Buzsaki G. Theta rhythm of navigation: Link between path integration and landmark navigation, episodic and semantic memory. Hippocampus. 2005; 15(7):827–840. [PubMed: 16149082]

Cantero JL, Atienza M, Stickgold R, Kahana MJ, Madsen JR, Kocsis B. Sleep-dependent θ oscillations in the human hippocampus and neocortex. J Neurosci. 2003; 23(34):10897–10903. [PubMed: 14645485]

Caplan JB, Madsen JR, Schulze-Bonhage A, Aschenbrenner-Scheibe R, Newman EL, Kahana MJ. Human θ oscillations related to sensorimotor integration and spatial learning. J Neurosci. 2003; 23(11):4726–4736. [PubMed: 12805312]

Cornwell BR, Johnson LL, Holroyd T, Carver FW, Grillon C. Human hippocampal and parahippocampal theta during goal-directed spatial navigation predicts performance on a virtual Morris water maze. J Neurosci. 2008; 28(23):5983–5990. [PubMed: 18524903]

Cornwell BR, Salvadore G, Colon-Rosario V, Latov DR, Holroyd T, Carver FW, Coppola R, Manji HK, Zarate CA Jr, Grillon C. Abnormal hippocampal functioning and impaired navigation in depressed individuals: Evidence from whole-head magnetoencephalography. Am J Psychiatry. 2010; 167:836–844. [PubMed: 20439387]

Cox RW. AFNI: Software for analysis and visualization of functional magnetic resonance neuroimages. Comput Biomed Res. 1996; 29:162–173. [PubMed: 8812068]

Czerniawski J, Yoon T, Otto T. Dissociating space and trace in dorsal and ventral hippocampus. Hippocampus. 2009; 19(1):20–32. [PubMed: 18651617]

Davidson TL, Jarrard LE. The hippocampus and inhibitory learning: a 'Gray' area? Neurosci Biobehav Rev. 2004; 28:261–271. [PubMed: 15225970]

de Araújo DB, Baffa O, Wakai RT. Theta oscillations and human navigation: A magnetoencephalography study. J Cogn Neurosci. 2002; 14(1):70–78. [PubMed: 11798388]

Duzel E, Penny WD, Burgess N. Brain oscillations and memory. Curr Opin Neurobiol. 2010; 20(2): 143–149. [PubMed: 20181475]

Eichenbaum H. Hippocampus: cognitive processes and neural representations that underlie declarative memory. Neuron. 2004; 44:109–120. [PubMed: 15450164]

Ekstrom AD, Caplan JB, Ho E, Shattuck K, Fried I, Kahana MJ. Human hippocampal theta activity during virtual navigation. Hippocampus. 2005; 15:881–889. [PubMed: 16114040]

Fanselow MS, Dong H-W. Are the dorsal and ventral hippocampus functionally distinct structures? Neuron. 2010; 65:7–19. [PubMed: 20152109]

First, MB.; Spitzer, RI.; Williams, JBW.; Gibbon, M. Structured clinical interview for DSM-IV (SCID). Washington, DC: American Psychiatry Association; 1995.

Fortin M, Voss P, Lord C, Lassonde M, Pruessner J, Saint-Amour D, Rainville C, Lepore F. Wayfinding in the blind: larger hippocampal volume and supranormal spatial navigation. Brain. 2008; 131:2995–3005. [PubMed: 18854327]

Frodl TS, Koutsouleris N, Bottlender R, Born C, Jager M, Scupin I, Reiser M, Moller HJ, Meisenzahl EM. Depression-related variation in brain morphology over 3 years. Arch Gen Psychiatry. 2008; 65:1156–1165. [PubMed: 18838632]

Furey ML, Khanna A, Hoffman EM, Drevets WC. Scopolamine produces larger antidepressant and antianxiety effects in women than in men. Neuropsychopharmacol. 2010; 35:2479–2488.

Gomez A, Rousset S, Baciu M. Egocentric-updating during navigation facilitates episodic memory retrieval. Acta Psychol (Amst). 2009; 132(3):221–227. [PubMed: 19664742]

Goodrich-Hunsaker NJ, Livingstone SA, Skelton RW, Hopkins RO. Spatial deficits in a virtual water maze in amnesic participants with hippocampal damage. Hippocampus. 2010; 20(4):481–491. [PubMed: 19554566]

Gordon JA, Lacefield CO, Kentros CG, Hen R. State-dependent alterations in hippocampal oscillations in serotonin 1A receptor-deficient mice. J Neurosci. 2005; 25(28):6509–6519. [PubMed: 16014712]

Gray, J.; McNaughton, N. The Neuropsychology of Anxiety: an Enquiry into the Functions of the Septo-hippocampal System. Second Edition. Oxford: Oxford University Press; 2000.

Grön G, Wunderlich AP, Spitzer M, Tomczak R, Riepe MW. Brain activation during human navigation: gender-different neural networks as substrate of performance. Nat Neurosci. 2000; 3:404–408. [PubMed: 10725932]

Grillon C. Startle reactivity and anxiety disorders: aversive conditioning, context, and neurobiology. Biol Psychiatry. 2002; 52(10):958–975. [PubMed: 12437937]

Hartley T, Maguire EA, Spiers HJ, Burgess N. The well-worn route and the path less traveled: distinct neural bases of route following and wayfinding in humans. Neuron. 2003; 37:877–888. [PubMed: 12628177]

Hasler G, Fromm S, Alvarez RP, Luckenbaugh DA, Drevets WC, Grillon C. Cerebral blood flow in immediate and sustained anxiety. J Neurosci. 2007; 27(23):6313–6319. [PubMed: 17554005]

Henneman WJP, Sluimer JD, Barnes J, van der Flier WM, Sluimer IC, Fox NC, Scheltens P, Vrenken H, Barkhof F. Hippocampal atrophy rates in Alzheimer disease: Added value over whole brain volume measures. Neurology. 2009; 72(11):999–1007. [PubMed: 19289740]

Hillebrand A, Singh KD, Holliday IE, Furlong PL, Barnes GR. A new approach to neuroimaging with magnetoencephalography. Hum Brain Mapp. 2005; 25:199–211. [PubMed: 15846771]

Iglói K, Doeller CF, Berthoz A, Rondi-Reig L, Burgess N. Lateralized human hippocampal activity predicts navigation based on sequence or place memory. Proc Natl Acad Sci USA. 2010; 107:14466–14471. [PubMed: 20660746]

Ishikawa A, Nakamura S. Ventral hippocampal neurons project axons simultaneously to the medial prefrontal cortex and amygdala in the rat. J Neurophysiol. 2006; 96(4):2134–2138. [PubMed: 16837666]

Jacobs J, Kahana MJ, Ekstrom AD, Fried I. Brain oscillations control timing of single-neuron activity in humans. J Neurosci. 2007; 27:3839–3844. [PubMed: 17409248]

Jacobs J, Korolev IO, Caplan JB, Ekstrom AD, Litt B, Baltuch G, Fried I, Schulze-Bonhage A, Madsen JR, Kahana MJ. Right-lateralized brain oscillations in human spatial navigation. J Cogn Neurosci. 2010; 22(5):824–836. [PubMed: 19400683]

Jung MW, Wiener SI, McNaughton BL. Comparison of spatial firing characteristics of units in dorsal and ventral hippocampus of the rat. J Neurosci. 1994; 14:7347–7356. [PubMed: 7996180]

Kahana MJ, Seelig D, Madsen JR. Theta returns. Curr Opin Neurobiol. 2001; 11(6):739–744. [PubMed: 11741027]

Karl A, Schaefer M, Malta LS, Dorfel D, Rohleder N, Werner A. A meta-analysis of structural brain abnormalities in PTSD. Neurosci Biobehav Rev. 2006; 30(7):1004–1031. [PubMed: 16730374]

Kjelstrup KB, Solstad T, Brun VH, Hafting T, Leutgeb S, Witter MP, Moser EI, Moser MB. Finite scale of spatial representation in the hippocampus. Science. 2008; 321:140–143. [PubMed: 18599792]

Kjelstrup KG, Tuvnes FA, Steffenach HA, Murison R, Moser EI, Moser MB. Reduced fear expression after lesions of the ventral hippocampus. Proc Natl Acad Sci USA. 2002; 99:10825–10830. [PubMed: 12149439]

Klur S, Muller C, de Vasconcelos AP, Ballard T, Lopez J, Galani R, Certa U, Cassel J-C. Hippocampal-dependent spatial memory functions might be lateralized in rats: An approach combining gene expression profiling and reversible inactivation. Hippocampus. 2009; 19:800–816. [PubMed: 19235229]

Lancaster JL, Woldorff MG, Parsons LM, Liotti M, Freitas CS, Rainey L, Kochunov PV, Nickerson D, Mikiten SA, Fox PT. Automated Talairach atlas labels for functional brain mapping. Hum Brain Mapp. 2000; 10:120–131. [PubMed: 10912591]

Lega BC, Jacobs J, Kahana M. Human hippocampal theta oscillations and the formation of episodic memories. Hippocampus. 2011

Maguire EA, Burgess N, Donnett JG, Frackowiak RSJ, Frith CD, O'Keefe J. Knowing where, and getting there: a human navigation network. Science. 1998; 280:921–924. [PubMed: 9572740]

Maguire EA, Burgess N, O'Keefe J. Human spatial navigation: cognitive maps, sexual dimorphism, and neural substrates. Cur Opin Neurobiol. 1999; 9:171–177.

Marshner A, Kalisch R, Vervliet B, Vansteenwegen D, Büchel C. Dissociable roles for the hippocampus and the amygdala in human cued versus context fear conditioning. J Neurosci. 2008; 28(36):9030–9036. [PubMed: 18768697]

McNaughton N, Ruan M, Woodnorth M-A. Restoring theta-like rhythmicity in rats restores initial learning in the Morris water maze. Hippocampus. 2006; 16:1102–1110. [PubMed: 17068783]

McNaughton N, Kocsis B, Hajos M. Elicited hippocampal theta rhythm: a screen for anxiolytic and precognitive drugs through changes in hippocampal function? Behav Pharmacol. 2007; 18:329–346. [PubMed: 17762505]

McNaughton N, Sedgwick EM. Reticular stimulation and hippocampal theta rhythm in rats: effects of drugs. Neuroscience. 1978; 3:629–632. [PubMed: 724111]

Moita MAP, Rosis S, Zhou Y, LeDoux JE, Blair HT. Putting fear in its place: Remapping of hippocampal place cells during fear conditioning. J Neurosci. 2004; 24(31):7015–7023. [PubMed: 15295037]

Mormann F, Osterhage H, Andrzejak RG, Weber B, Fernandez G, Fell J, Elger CE, Lehnertz K. Independent delta/theta rhythms in the human hippocampus and entorhinal cortex. Front Hum Neurosci. 2008; 2:3. [PubMed: 18958204]

Morris RGM, Garrud P, Rawlins JN, O'Keefe J. Place navigation impaired in rats with hippocampal lesions. Nature. 1982; 297:681–683. [PubMed: 7088155]

Moser E, Moser MB, Andersen P. Spatial learning impairment parallels the magnitude of dorsal hippocampal lesions, but is hardly present following ventral lesions. J Neurosci. 1993; 13(9): 3916–3925. [PubMed: 8366351]

Moser MB, Moser EI, Forrest E, Andersen P, Morris RG. Spatial learning with a minislab in the dorsal hippocampus. Proc Natl Acad Sci USA. 1995; 92(21):9697–9701. [PubMed: 7568200]

Moses SN, Ryan JD, Bardouille T, Kovacevic N, Hanlon FM, McIntosh AR. Semantic information alters neural activation during transverse patterning performance. NeuroImage. 2009; 46(3):863–873. [PubMed: 19281852]

Ohmura Y, Izumi T, Yamaguchi T, Tsutsui-Kimura I, Yoshida T, Yoshioka M. The serotonergic projection from the median raphe nucleus to the ventral hippocampus is involved in the retrieval of fear memory through the corticotrophin-releasing factor type 2 receptor. Neuropsychopharmacol. 2010; 35:1271–1278.

O'Keefe, J.; Nadel, L. The hippocampus as a cognitive map. Oxford: Oxford University Press; 1978.

Oler JA, Fox AS, Shelton SE, Rogers J, Dyer TD, Davidson RJ, Shelledy W, Oakes TR, Blangero J, Kalin NH. Amygdalar and hippocampal substrates of anxious temperament differ in their heritability. Nature. 2010; 466:864–868. [PubMed: 20703306]

Pape H-C, Narayanan RT, Smid J, Stork O, Seidenbecher T. Theta activity in neurons and networks of the amygdala related to long-term fear memory. Hippocampus. 2005; 15:874–880. [PubMed: 16158424]

Quraan MA, Moses SN, Hung Y, Mills T, Taylor MJ. Detection and localization of hippocampal activity using beamformers with MEG: A detailed investigation using simulations and empirical data. Hum Brain Mapp. 2010

Royer S, Sirota A, Patel J, Buzsaki G. Distinct representations and theta dynamics in dorsal and ventral hippocampus. J Neurosci. 2010; 30(5):1777–1787. [PubMed: 20130187]

Riggs L, Moses SN, Bardouille T, Herdman AT, Ross B, Ryan JD. A complementary analytic approach to examining medial temporal lobe sources using magnetoencephalography. NeuroImage. 2009; 45(2):627–642. [PubMed: 19100846]

Sahay A, Hen R. Adult hippocampal neurogenesis in depression. Nat Neurosci. 2007; 10:1110–1115. [PubMed: 17726477]

Sainsbury RS, Heynen A, Montoya CP. Behavioral correlates of hippocampal type 2 theta in the rat. Physiol Behav. 1987; 39:513–519. [PubMed: 3575499]

Sainsbury RS, Montoya CP. The relationship between type 2 theta and behavior. Physiol Behav. 1984; 33(4):621–626. [PubMed: 6522481]

Salehi B, Cordero MI, Sandi C. Learning under stress: the inverted-U-shape function revisited. Learn Mem. 2010; 17(10):522–530. [PubMed: 20884754]

Schwabe L, Oitzl MS, Philippsen C, Richter S, Bohringer A, Wippich W, Schachinger H. Stress modulates the use of spatial versus stimulus-response learning strategies in humans. Learn Mem. 2007; 14:109–116. [PubMed: 17272656]

Seidenbecher T, Laxmi TR, Stork O, Pape H-C. Amygdalar and hippocampal theta rhythm synchronization during fear memory retrieval. Science. 2003; 301(5634):846–850. [PubMed: 12907806]

Shin J. Theta rhythm heterogeneity in humans. Clin Neurophysiol. 2009; 121:453–457. [PubMed: 20005162]

Shin J, Gireesh G, Kim S-W, Kim D-S, Lee S, Kim Y-S, Watanabe M, Shin H-S. Phospholipase C β4 in the medial septum controls cholinergic theta oscillations and anxiety behaviors. J Neurosci. 2009; 29(49):15375–15385. [PubMed: 20007462]

Shin J, Kim D, Bianchi R, Wong R-W, Shin H-S. Genetic dissection of theta rhythm heterogeneity in mice. Proc Natl Acad Sci USA. 2005; 102:18165–18170. [PubMed: 16330775]

Stewart M, Fox SE. Hippocampal theta activity in monkeys. Brain Res. 1991; 538(1):59–63. [PubMed: 2018932]

Stockwell RG, Mansinha L, Lowe RP. Localization of the complex spectrum: The S transform. IEEE Trans Sign Process. 1996; 44:998–1000.

Vanderwolf CH. Neocortical and hippocampal activation relation to behavior: effects of atropine, eserine, phenothiazines, and amphetamine. J Comp Physiol Psychol. 1975; 88(1):300–323. [PubMed: 235571]

Vrba J, Robinson SE. Signal processing in magnetoencephalography. Methods. 2001; 25(2):249–271. [PubMed: 11812209]

Winson J. Loss of hippocampal theta rhythm results in spatial memory deficit in the rat. Science. 1978; 201:160–163. [PubMed: 663646]

Wolbers T, Büchel C. Dissociable retrosplenial and hippocampal contributions to successful formation of survey representations. J Neurosci. 2005; 25:3333–3340. [PubMed: 15800188]

Woollett K, Maguire EA. Navigational expertise may compromise anterograde associative memory. Neuropsychologia. 2009; 47:1088–1095. [PubMed: 19171158]

Woolley DG, Vermaercke B, de Beeck HO, Wagemans J, Gantois I, D'Hooge R, Swinnen SP, Wenderoth N. Sex differences in human virtual water maze performance: Novel measures reveal the relative contribution of directional responding and spatial knowledge. Behav Brain Res. 2010; 208:408–414. [PubMed: 20035800]

Xu J, Evensmoen HR, Lehn H, Pintzka CWS, Haberg AK. Persistent posterior and transient anterior medial temporal lobe activity. NeuroImage. 2010; 52:1654–1666. [PubMed: 20677377]

Yerkes RM, Dodson JD. The relation of strength of stimulus to rapidity of habit-formation. J Comp Neurol. 1908; 18:459–482.

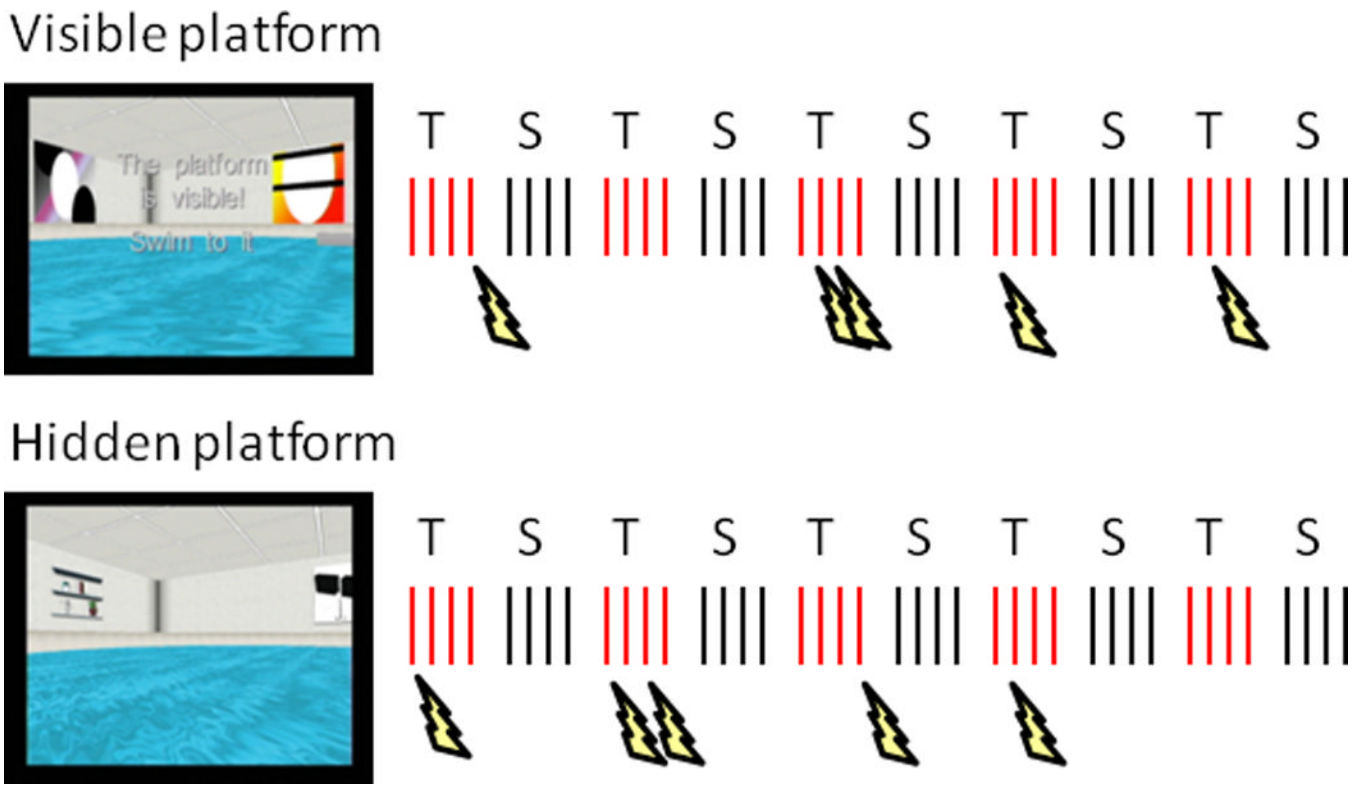

Figure 1.
Diagram of the virtual Morris water maze task. Two runs of 40 trials were completed, half during threat of shock (T) in one pool environment and half during safety (S) in another pool environment. The platform was visible or above the water in the first run, and hidden or submerged in the same location in the second run. Participants completed a block of 4 trials (red and black hash marks) within a pool before alternating to the other, starting from each of four random locations at the pool's edge. In the threat pool, shocks (lightning bolts) were delivered on 5 different trials per run.

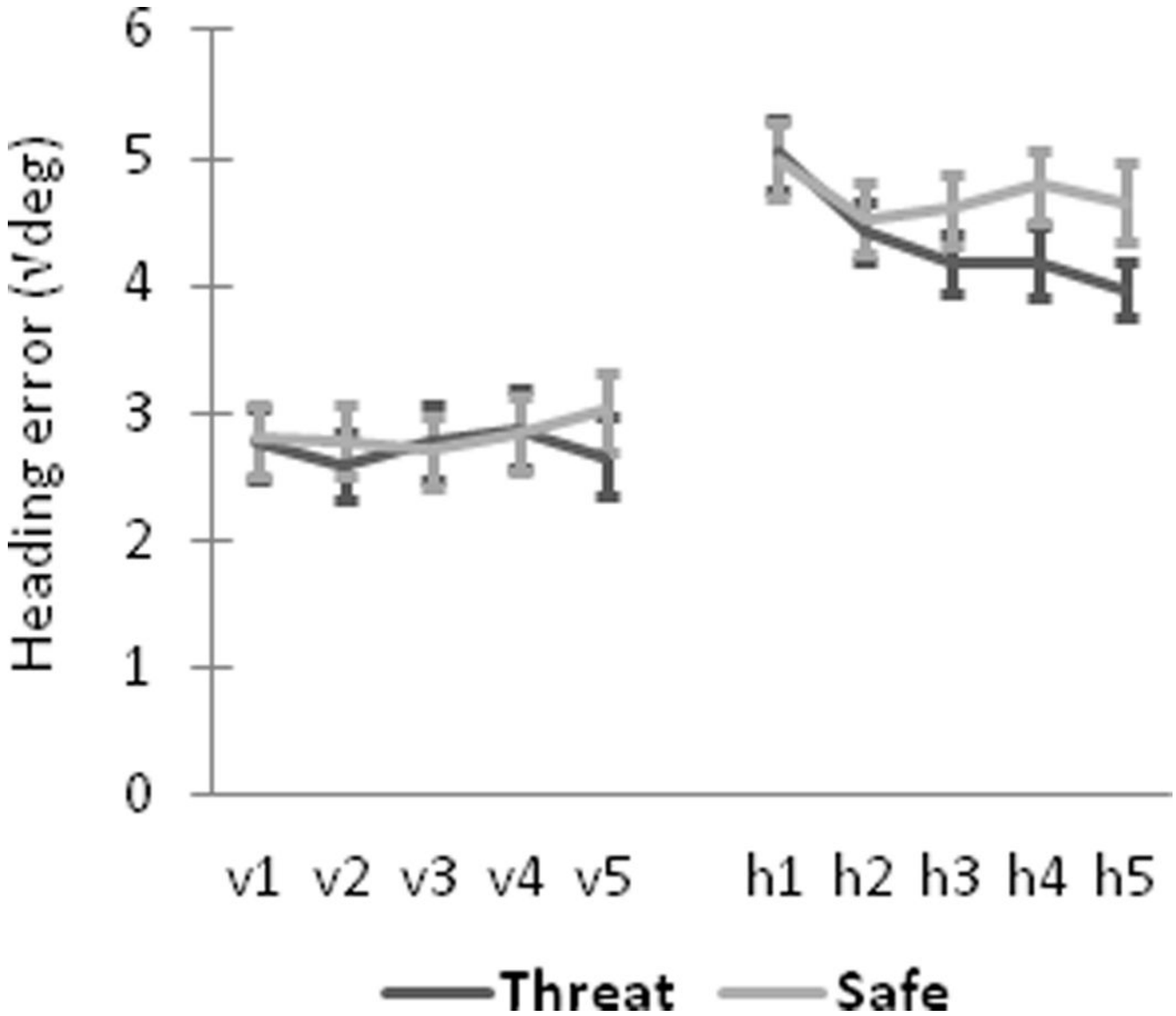

Figure 2.
Enhanced spatial navigation to the hidden platform during threat. Mean heading error (square-root transformed) for threat and safe conditions is shown for visible platform trials (v1–v5), hidden platform trials (h1–h5). Error bars represent standard errors of the mean.

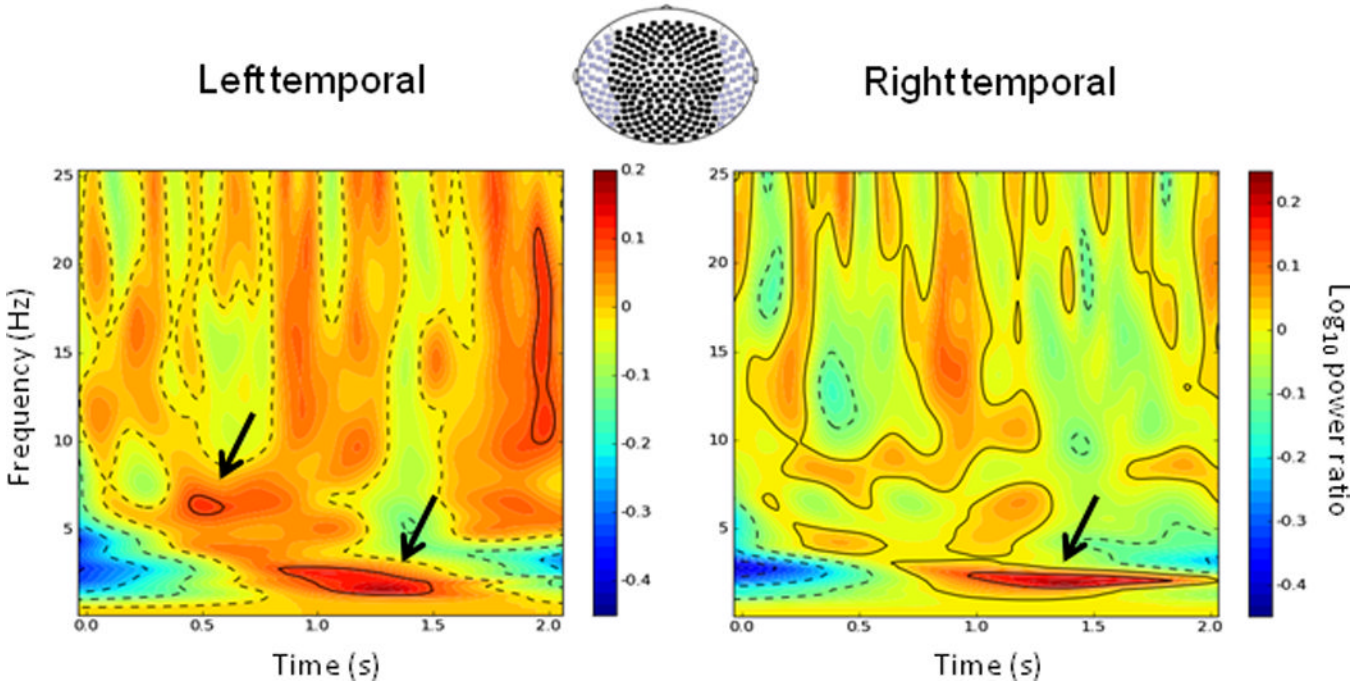

Figure 3.

Induced spectral differences in navigation-related oscillatory activity between threat and safe conditions. Grand-averaged (N = 25) time-frequency plots of differential navigation-related activity (threat - safe) for the hidden platform run. Data are unsmoothed and normalized to a 1-s baseline period (not shown). The first 2 seconds of the trial is averaged for sensors (axial gradiometers) overlying left and right temporal cortices separately (purple-colored in the sensor array). Arrows highlight two peak spectral differences in the theta band between threat and safe conditions. Time is relative to trial onset.

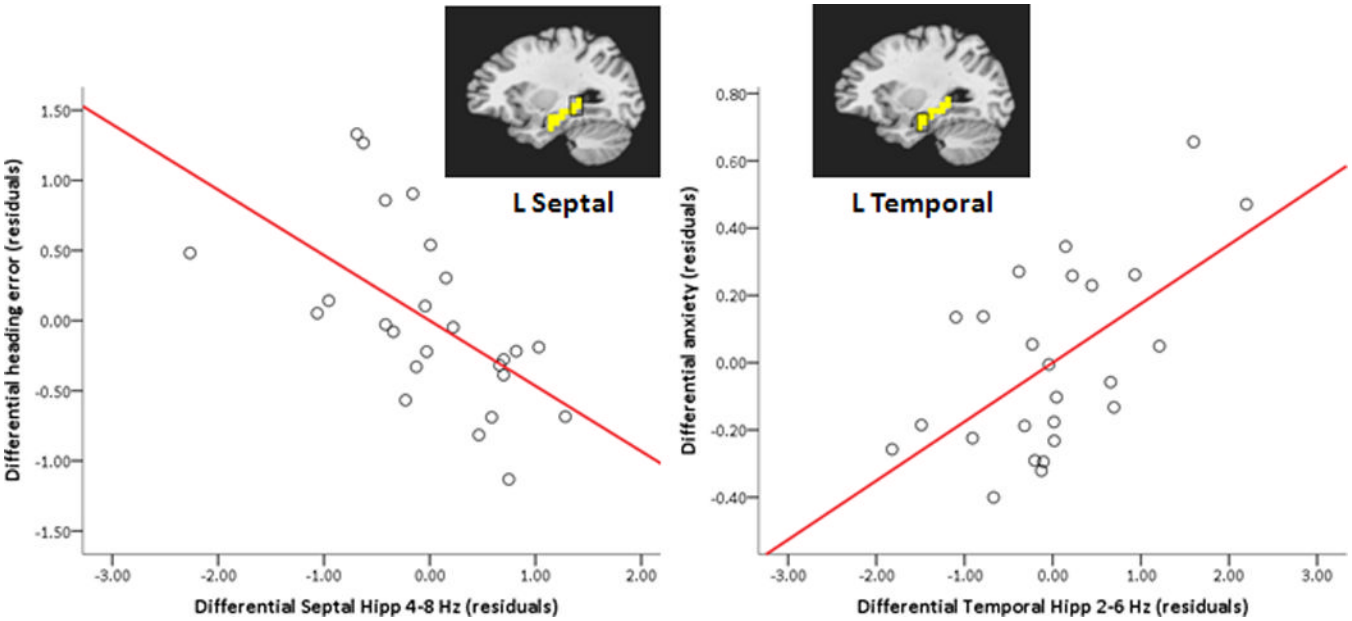

Figure 4.

Hippocampal region-of-interest (ROI) theta predicts navigation performance and anxiety level. Partial regression plots (with least square lines) show relationships between differential (threat – safe) left hippocampal ROI high theta (4–8 Hz) and differential heading error (left), and between differential left hippocampal ROI low theta (2–6 Hz) and differential anxiety in the hidden platform condition (right). A mask of the left hippocampus (in yellow) is overlayed on a standardized brain, highlighting septal and temporal thirds of the hippocampus from which data were extracted for regression analyses. Note that smaller differential heading errors reflect better performance during threat relative to safe conditions. Hipp = hippocampus; L = left.